

Fabrication and characterization of highly efficient dye-sensitized solar cells with composited dyes

G. H. C. Radloff, F. M. Naba, D. B. Ocran-Sarsah, M. E. Bennett,

K. M. Sterzinger, A. T. Armstrong, O. Layne, M. B. Dawadi*

Department of Chemistry and Biochemistry, Earlham College, 801 National Rd W, Richmond, IN, 47374

As a representative of the next-generation solar cells, dye-sensitized solar cells (DSSCs) offer the efficient and ease of implementation of new technology for future energy supply. Herein, four commercially available dyes including, curcumin (C), betanin (B), crystal violet (CV), and methylene blue (MB), and their compositions were used as sensitizers for fabrication of titanium oxide photo-anode based DSSCs. All dyes were fully characterized using absorption and emission spectroscopy. Both DFT and TDDFT studies were also carried out to probe the electronic structure of these dyes. The power conversion efficiencies of each DSSCs prepared using the individual and composited dyes were measured and compared. Particularly, this is the first study to combine four different dyes for DSSCs, leading to a remarkable increase of power conversion efficiency. The DSSCs with combined curcumin, betanin, crystal violet, and methylene blue (in ratio 1:1:1:1 respectively) in ethanol exhibited the highest power conversion efficiency of 3.63%.

(Received December 20, 2021; Accepted April 4, 2022)

Keywords: Dye-sensitized solar cells (DSSCs), Density functional theory (DFT), Sensitizers, Power conversion efficiency (PCE), Current-voltage (I-V) characteristics

1. Introduction

As nonrenewable sources of energy become expended, the need for an alternative, renewable source of energy becomes greater by the day [1, 2]. The greatest replacement for these high energy producing materials would be the sun, and being able to harness the solar irradiance would undoubtedly solve the energy crisis [3]. Photovoltaic devices, so-called solar cells, are promising technologies to convert solar energy into electrical energy in which the photocurrent is generated through charge separation and collection of free electron and hole under solar irradiation [4]. Over the past years, various types of solar cells, including crystalline, polycrystalline, amorphous, and multijunction semiconductor solar cells, have been widely used for different domestic and industrial applications [5]. However, the cost of these solar cells necessary for the conversion of sunlight to electricity remains the largest barrier toward the more widespread implementation of solar energy as a long-term solution to the impending energy crisis [3, 6].

Dye-sensitized solar cells (DSSCs) have been demonstrated as one of the representatives of the third-generation of photovoltaic devices [7-9] developed by O'Regan and Gratzel in 1991[10], and have broad applications in solar-powered windows [11, 12] and as passive energy harvesters in wearable devices and textiles [13, 14]. DSSCs convert photon from solar energy to electrical energy based on sensitization of dyes and electrolytes. They are environmentally and economically attractive because of their ease of fabrication, low manufacturing cost (leading to production of less expensive cells in large volumes), lightweight, abundance of their starting materials, small environmental footprint, being able to be designed in a wide range of shapes, sizes, colors and transparencies, and relatively high-power conversion efficiency (PCE) [4, 6]. A typical DSSC, as shown in Fig. 1, consist of two transparent electrodes; working electrodes and counter electrodes, and an organic-based redox electrolyte system, placed between the two

* Corresponding author: dawadma@earlham.edu
<https://doi.org/10.15251/DJNB.2022.172.457>

electrodes, is usually an organic system containing redox couple, i.e. the iodide/iodine redox couple (I^-/I_3^-). The operation of a DSSC involves multistep processes. Initially, organic dye molecule absorbs the photon of sun light and gets excited. This photo-excitation of organic dye results in the injection of an electron into the conduction band (CB) of TiO_2 , thus leaving the sensitizer in the oxidized state. Then, regeneration of oxidized sensitizer is accompanied by accepting electrons from the organic electrolytic system. Thus, the entire cycle is regenerative.

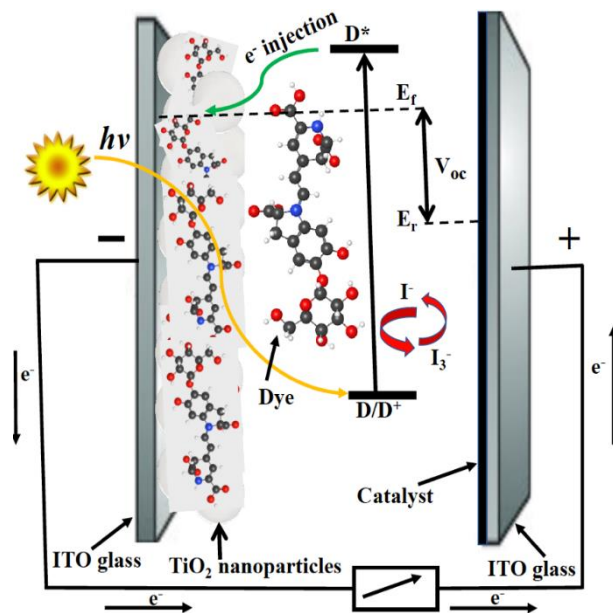


Fig. 1. Schematic diagram of a typical dye-sensitized solar cell.

The performance of the DSSCs mainly depends on the sensitizer dye, plays the role of light harvester and electron transfer agent, like the chlorophyll in natural photosynthesis, wide band gap semiconductors such as TiO_2 , SnO_2 , ZnO and Nb_2O_5 [15]. In recent years titanium dioxide (TiO_2) has attracted attention worldwide due to its potential applications in sustainability, environmental protection, and energy generation [16], and has also been applied largely in DSSC due to its nanocrystalline mesoporous nature that translates to high surface area for dye adsorption [10]. In general, the performance of dye absorption on the surface of working electrodes (dye-coated semiconductors) determines the efficiency of the solar cell [17]. DSSCs fabricated using nanocrystalline TiO_2 films sensitized with ruthenium complex dyes (N719) have achieved the highest power conversion efficiency of 10-12% [18-20]. However, ruthenium-based complexes are very expensive and lack long-term stability which limits their large-scale applications in solar cells [19]. This encourages investigation of low cost, readily available alternatives such as organic dyes as efficient sensitizer for DSSCs [20, 21]. However, some of the major parameters including electrolyte leakage, dye desorption, degradation, and lack of broad range of absorption spectrum of dyes affect the long-term stability of DSSCs [22, 23].

The DSSC device is an ensemble of various materials that undergo different interactions and processes, and researchers have been focusing on the optimization of the several working components of the DSSC with the aim to obtain maximum power conversion efficiency. For example, the effect of drying and thickness of TiO_2 onto ITO (Indium tin oxide) and its annealing conditions on photovoltaic devices responses [24, 25], and the quality of photosensitizer and its photon harvesting ability have been widely studied. Additionally, a mixture of dye molecules has been used as a photosensitizer, responsible for solar energy caption, to allow wider optically active photon absorption range in the UV-Visible region of the solar spectrum to absorb more photons from the sunlight. A number of organic molecules can absorb quite a vital part of the solar visible spectrum (400-700 nm), which accounts for 60% of the whole solar energy spectrum. Absorption

of more photons of energy in a wider range in the UV-visible region is leading to an increase in more efficient incident photon-to-electron conversion efficiency [4, 20, 26].

In this work, we report the first study to fabricate a novel type of DSSC by co-sensitizing it with combination of four different dyes, including curcumin (C), betanin (B), crystal violet (CV), and methylene blue (MB) (Fig. 2) in two solvents (water and ethanol). The use of the combination of dyes as a sensitizer in DSSCs helps to cover the extended light absorption throughout the visible region of the solar spectrum. This increases the power conversion efficiency of the devices. Additionally, the performance of new DSSCs fabricated using the mixture of sensitizers are compared with the DSSCs fabricated with individual dyes. Furthermore, they were fully characterized using absorption and emission spectroscopy, electronic structure density function theory (DFT/TDDFT) calculation, and performance tests. We found that the combination of four dyes for DSSCs in ethanol can remarkably increase the power conversion efficiency.

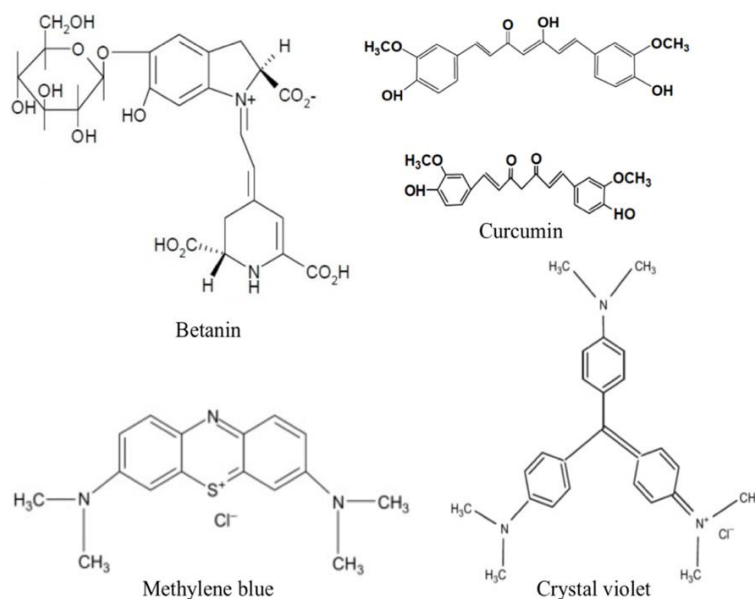


Fig. 2. Structure of organic dyes: curcumin (enol and keto), betanin, methylene blue and crystal violet.

2. Experimental Section

2.1. Materials and Instruments

Curcumin, betanin, crystal violet, methylene blue, ethanol, DMSO, sodium hydroxide, P25 TiO₂ nano-powder, titanium isopropoxide, Triton X 100, potassium iodide, iodine, polyethylene glycol, and indium doped tin oxide (ITO) glass were purchased from Sigma Aldrich, Inc. Turmeric and red beet root were purchased from the local vegetable market. The UV-visible absorption spectra of all samples was measured using a UV-visible diode array spectrophotometer. The steady-state emission spectra were recorded using Spectrofluorometer F55. Quartz cuvettes were used for loading the sample into both the spectrometer and fluorometer. The photovoltaic performance of fabricated DSSCs was measured under AM 1.5G standard conditions (100 mW/cm²) at room temperature, using a handmade class A small area solar simulator [27]. Temperature controller was used to maintain constant temperature throughout the process. The current and voltage values were measured using two digital bench multimeters and a decadic resistance box without any external bias. All measurements were made at intervals of ~10 s, allowing for each reading to stabilize.

2.2. Preparation of Dye Solutions

All the solvents and the chemicals employed for the experiments were of reagent or spectrophotometric grade. Four ~ 0.6 M dyes solutions (curcumin, betanin, crystal violet, and

methylene blue in ratio 1:1:1:1) were prepared separately using water and ethanol as the solvents. Initially, each of these dye solutions were used as a photosensitizer in the DSSCs. Then, the mixture of these dyes was used as the sensitizer in the DSSCs.

The method of extraction changed depending on the plant being broken down and the solvent used to extract the pigment. The raw plants / vegetable material to extract natural dyes was obtained locally and easily. For the preparation of the red beetroot solution in H₂O, about 30mg of red beetroot was ground using mortar and pestle. Once the beetroot was the consistency of a smoothie, small amounts of DI H₂O were added to dissolve the dye. Once about 20mL was added, the solution was filtered. Similarly, for the preparation of the red beetroot solution in ethanol, about 30mg of red beetroot was ground using mortar and pestle. Once the beetroot was the consistency of a smoothie, it was put in an oven at about 105°C to allow much of the water found in the root to evaporate. After 30 minutes, the root slurry was removed from the oven, and about 25mL of ethanol was added and mixed thoroughly. Once the solution was filtered, about 27 mL of liquid was present, so the solution was about 93% ethanol. However, for the turmeric solution, we use the traditional method in which a small amount of turmeric was crushed by mortar pestle using various solvent such as water and ethanol separately. The solvents were added over the small pieces of clean red beetroots and turmeric (10 mL of solvent for each 1 g of the sample). Then, each extract was filtered and used as the sensitizer source. All dye solutions were wrapped in aluminum foil and stored in a dark space in between uses to protect from direct light exposure.

2.3. Dye-sensitized solar cell Fabrication

Conducting indium-doped tin oxide (ITO) glass plates were used as substrates for depositing TiO₂ porous films after being cleaned. These plates were ultrasonically washed for a total of 30 minutes, ten minutes each, separately, with acetone, ethanol, and distilled water with acetone, alcohol, and distilled water. The conductive side of the glass plate was determined by touching the protruding leads of the multi-meter to one side of the glass. The conductive side of the glass plate has an average resistance of 20-38 ohms. The plates were then heated on their conductive side for 30 min at 500 °C. The TiO₂ paste was prepared by adding dilute acetic acid/vinegar to 1 g of TiO₂ powder. This was ground in a mortar and pestle until a paste with a smooth consistency (like cake icing) was observed, and then, added two drops of a diluted solution of Triton X-100 on it. The paste was added to form a TiO₂ film on ITO by the doctor-blade method. A Scotch adhesive tape (50 μm thickness) was used as the masking material for the doctor-blading method. Subsequently, the tape was removed from the glass plate without scattering the TiO₂ layer. This TiO₂ film coated plate was initially dried under room temperature then gradually heated under an air flow at at 375° C for 5 minutes followed by 400 °C for 5 min, then 15 min at 450° C and 500° C consequently. This TiO₂/ITO glass plate was soaked in the ~0.6 M dye solution for ~24 h to achieve dye sensitization. Another carbon coated ITO glass plate was employed for counter electrode.

2.4. Preparation of electrolyte and assembly of DSSCs

The electrolyte solution for the DSSCs was prepared by dissolving KI (0.5 M) and I₂ (0.05 M) in mixed solvents of ethylene glycol and acetonitrile (4:1 in the volume ratio) [28]. Photo-anode and counter electrode were then clamped together using two binder clips. The iodide electrolyte solution was added drop wise onto the interface between the two photo-electrodes. The electrolyte was drawn into the space between the electrodes by capillary action.

2.5 Characterization of dye-sensitized solar cells (DSSCs)

The power conversion efficiency for (i) single-dye sensitized solar cells and (ii) mixture of dyes-sensitized solar cells in water and ethanol were characterized and compared with each other to optimize the designs of DSSCs. We used ~0.6 M concentration of the individual dye sample to measure the power conversion efficiency [4]. Additionally, the power conversion efficiencies of different combinations of curcumin, betanin, crystal violet, and methylene blue (in ratio 1:1:1:1) in water and ethanol, were compared to find the optimum conditions for the combination dyes. The electro-optical parameters of the fabricated DSSCs, the short circuit current, I_{SC} , the open circuit

voltage, V_{OC} , the fill factor, FF , and the photovoltaic conversion efficiency, η , were characterized using a handmade solar simulator under a standard AM1.5G illumination condition of 100 mW/cm^2 . Temperature controller was used to maintain the constant temperature throughout the measurement process. The measurements were taken multiple times to check repeatability and the stability of the solar cells. The UV-visible absorption spectra of all samples was measured using a UV-visible diode array spectrophotometer. The steady-state emission spectra were recorded using Spectrofluorometer. Digital multimeters were used to measure J - V curves without external bias.

2.6. Computational Details

The structures of betanin, curcumin, crystal violet, and methylene blue dyes were optimized using Density Functional Theory (DFT) calculation [29], with the B3LYP exchange-correlation function [30, 31], and the 6-311+G (2d, p) basis set [32]. True energy minima in optimized geometries were confirmed by frequency calculations (no imaginary frequency). Water and ethanol were used as the solvents in all of the ground state DFT-PCM calculations and for the single point TDDFT-PCM calculations, solvent effects were calculated using the polarized continuum model (PCM) [33]. TDDFT calculations for the first ten singlet excitation energies were performed. All DFT calculations were performed using the Gaussian 16 computational Chemistry software package [34]. The results of these calculations help to consider the geometric and electronic parameters (HOMO level (highest occupied molecular orbital), LUMO (lowest unoccupied molecular orbital), the energy band gap (E_g), and the electronic transition energies)).

3. Results and discussion

3.1. Steady State Absorption Spectra of Individual Photosensitizer

The absorption spectra provide necessary information on the absorption transition between the ground state and excited states and the solar energy range absorbed by the dye molecule. Figure 3 shows the steady state absorption spectra of aqueous and ethanolic solutions of turmeric extract, curcumin, beetroot extract, betanin, crystal violet, and methylene blue respectively.

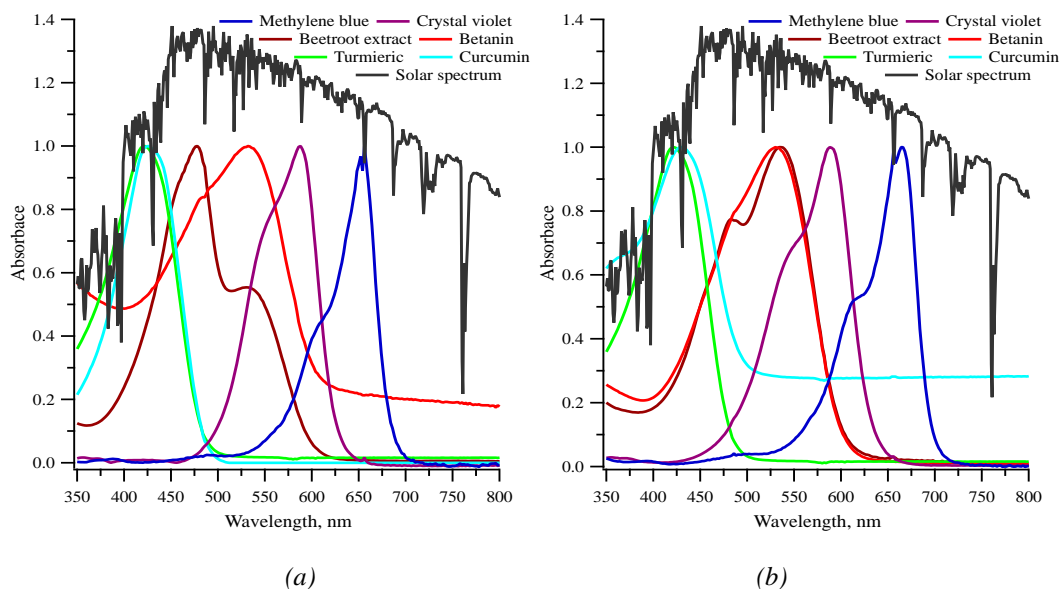


Fig. 3. UV-visible absorption spectra of beetroot extract, betanin, turmeric extract, curcumin, crystal violet, and methylene blue solutions (a) in water and (b) in ethanol, overlaid by the solar absorption spectrum for comparison.

The absorption band of dye molecules is solvent sensitive as depicted in Fig. 3. As shown in Fig. 3, aqueous solutions of curcumin, turmeric extract, betanin, red beetroot extract, crystal violet and methylene blue have absorption peak at 430, 422, 529, 530, 588, and 656 nm respectively, while ethanolic solutions have the absorption peak at 426, 420, 532, 478, 589, and 664 nm respectively. We found that the visible absorption bands of aqueous solutions of curcumin, turmeric extract, and red beetroot extract are red (bathochromic) shifted upon increasing the solvent polarity (ethanol \rightarrow water). However, the visible absorption bands of ethanolic solutions of betanin, crystal violet, and methylene blue are blue (hypsochromic) shifted upon increasing the solvent polarity (Figs. S1-S8). The absorbance of aqueous solution of curcumin was reported to be very weak, because curcumin is only slightly soluble in water. Additionally, the absorption spectrum of curcumin is a broad band with maximum absorption peak at \sim 430 (in water) or \sim 426 nm (ethanol), which could be assigned to low energy $\pi \rightarrow \pi^*$ excitation of the curcumin. Similarly, the absorption spectrum of betanin is also a broad band with maximum absorption peak at \sim 529 (in water) or \sim 532 nm (ethanol), which could be assigned to low energy $n \rightarrow \pi^*$ excitation of the betanin. These transitions ($\pi \rightarrow \pi^*$ and $n \rightarrow \pi^*$) are high-energy transitions that occur by absorption of the photon in the indigo and green wavelength range respectively, thus responsible for the yellowish and reddish color of curcumin and betanin respectively. In case of methylene blue, the absorption band with absorption peaks at \sim 656 nm (in water) or \sim 664 nm (in ethanol), which are characterized by the $n \rightarrow \pi^*$ transitions. These transitions ($n \rightarrow \pi^*$) are low-energy transitions that occur by the absorption of a photon in the red wavelength range, thus responsible for the blue color. Similarly, in crystal violet, the absorption band with absorption peaks at \sim 588 (in water) or 589 nm (in ethanol) are low energy transitions characterized by $n \rightarrow \pi^*$ transitions which occur by the absorption of a photon in the orange wavelength range, thus responsible for the violet color.

We found that there are significant differences between the absorption spectra of aqueous and ethanolic extracts of the red beetroots. In case of aqueous red beetroots extract solution, we found that there is a strong absorption band (or maximum absorbance) at \sim 530 nm, characteristic for the red-purple betacyanins (betanin), with a second higher energy and lower intensity peak to the blue at \sim 478 nm, characteristic for the yellow betaxanthins (indicaxanthin) (Fig. 3 and Fig. S6) [35]. However, for the ethanolic solution of the extract, we observed that the intensity of both absorbance bands is exactly opposite to that of the aqueous extract solution. In details, for the ethanolic extract solution, we observed that a strong (more intense) absorbance band at \sim 478 nm and a weak lower energy band at \sim 530 nm. This shows that natural red beetroots extract contains a mixture of several pigments and its composition depends on the type of solvent used in the extraction process. The concentration of betaxanthin, $[B_x]$ and betanin, $[B_n]$ present in the red beet roots extracts can be determined with the help of absorption spectrum, using equation 1 [36].

$$[B_x] = 23.8 Abs_{478} - 7.7 Abs_{530} \quad (1)$$

$$[B_n] = 15.38 Abs_{530}$$

We found that the concentration of $[B_x]$ and $[B_n]$ were \sim 10.7 μ M and 15.1 μ M, for the aqueous extract and 19.2 μ M and 8.2 μ M for the ethanolic extracts, respectively. This revealed that in the aqueous extract, the concentration of betanin, $[B_n]$, is higher than the concentration of betaxanthin, $[B_x]$, while in the ethanolic extract, the concentration of indicaxanthin, $[B_x]$ is higher than that of betanin, $[B_n]$.

3.2. Absorption spectra of mixed dyes as photosensitizers

One of the most important components of DSSC is the dye, which absorbs the photons of sunlight and injects the photoexcited electrons into the conduction band of the n -type semiconductor. To be an efficient sensitizer, it needs to fulfill stringent properties, such as harvesting light in a broad range of the solar spectrum ranging from visible to the near-infrared, bind strongly to the semiconductor nanoparticles, require a rapid regeneration by the electrolyte, and the energy of its electronic excited state should lie energetically above the CB of the TiO_2 [5,

6]. The absorption spectrum of a single dye hardly follows the whole solar spectrum (Fig. 3). So, an option to obtain an extended light absorption throughout the visible and near infra-red spectrum is to use the mixture of several dyes with different absorption spectral features [4]. For DSSCs applications, these mixtures co-sensitize the device to increase the global absorption using the wide wavelength range possible and hence maximizing the efficiency [20]. For this reason, we have studied the mixture of different dyes in both aqueous and ethanolic solutions in different proportions: curcumin and crystal violet solutions (1:1), betanin, and methylene blue solutions (1:1), and curcumin, betanin, crystal violet, and methylene blue solutions (1:1:1:1). Comparison of the spectra shows that the absorption spectra of four mixed dyes ((curcumin +betanin, +crystal violet + methylene blue) overlap broader range of the incident solar spectrum than the spectra of two mixed dyes (curcumin + crystal violet), (betanin + methylene blue) and the individual dyes (Figs. 3 and 4). As noted in Fig. 4, the absorbance peaks at ~ 426 , ~ 532 , ~ 589 , and ~ 660 nm (Fig. 4(b)) are characteristic peaks of ethanolic solutions of curcumin, betanin, crystal violet and methylene blue respectively. Additionally, we noted that the absorption spectrum of ethanolic solution of four mixed dyes is more intense and characteristic peaks of each dye is more prominent than absorption spectrum of aqueous solution (Figs. 4 (a) and (b)) due to the solubility effect. Thus, we predict that the higher power conversion efficiency for the co-sensitized solar cells using ethanolic solutions of four mixed dyes than for the aqueous counter parts, combination of two dyes, and individually co- sensitized solar cells. We did not include beetroots and turmeric extracts for this study.

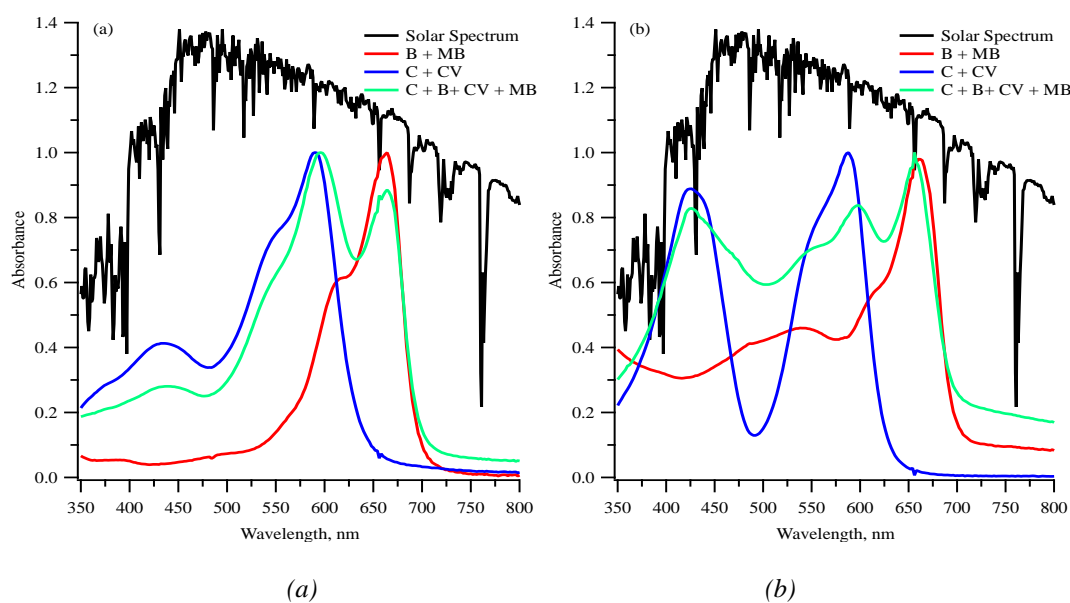


Fig. 4. UV-Visible absorption spectra of aqueous (a) and ethanolic (b) solutions of a mixture of curcumin (C), betanin (B), crystal violet (CV), and methylene blue (MB), overlaid by the solar absorption spectrum for comparison.

3.3. Fluorescence studies

Steady state fluorescence spectra of aqueous and ethanolic solution of all dyes were acquired as shown in Figs. 5 (a) and (b) demonstrates significant solvent dependent shifts in emission (fluorescence) maxima. We found that the fluorescence maxima of curcumin, betanin, crystal violet, and methylene blue red-shifted by 10 nm, 9 nm, 2 nm and 21 nm, respectively, after changing the solvent from water to ethanol, which indicates that the excited singlet state must be very polar. In case of curcumin in water, we observed that its fluorescence intensity was quenched. This quenching of fluorescence of curcumin in water can be attributed to a reaction between water (electron donor, D) and the fluorescence curcumin (C^*), resulting in the formation of a non-fluorescent and more stable complex (C^*D^+) with lower S_0 vibrational energy levels [37]. In

addition, we also observed that there is a broadening of fluorescence band for methylene blue after changing the solvent from water to ethanol (Fig.5).

We also compare the characteristic of fluorescence as a function of excitation wavelengths for both ethanolic and aqueous solutions of all dyes. We found that only ethanolic solution of curcumin and aqueous solution of betanin showed some characteristics spectroscopic features as a function of excitation wavelengths as shown in Fig.6. For the ethanolic solution of curcumin, fluorescence intensity decreases gradually as the excitation wavelength increases up to 430 nm excitation (Fig. 6 (a)). Interestingly, the emission maxima or peaks of these bands differed dramatically. As noted in Fig. 6 (a), the emission peaks were red shifted gradually as the excitation wavelength decreases from 430 nm to 350 nm (Fig. 6 (a)). Surprisingly, the fluorescence peaks blue shifted upon excitation of lower wavelengths (i.e., from 340-280 nm). We also observed that a weak and less distinct vibrational shoulder at ~ 500 nm appeared as a function of the excitation wavelength in the interval 390- 330 nm. This shoulder was completely vanished above and below this range of excitation wavelengths. We did not observe any spectroscopic features as a function of excitation wavelength for both the aqueous and ethanolic turmeric extract. For those cases, we found that fluorescence intensity gradually increases with the increase of excitation wavelength (Fig.7).

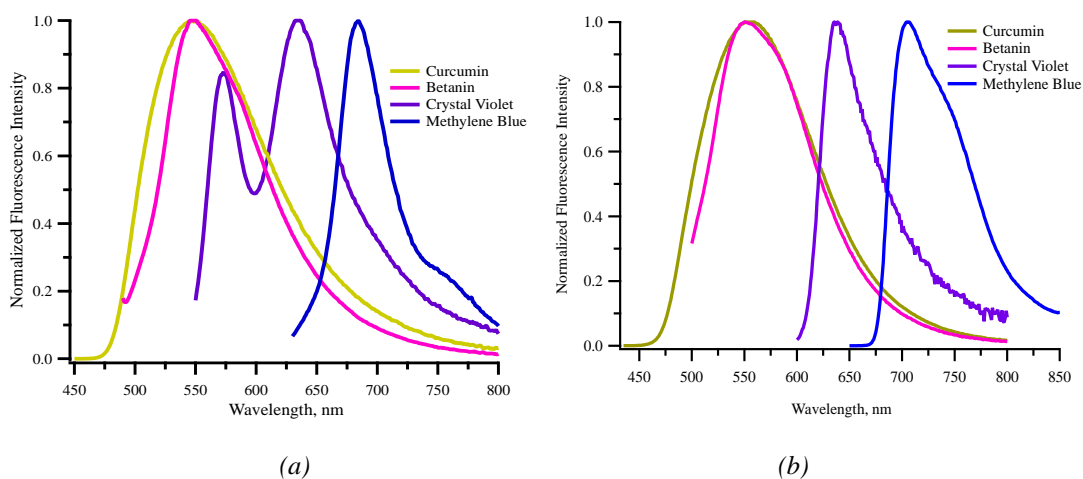


Fig.5. Fluorescence spectra of (a) aqueous and (b) ethanolic solutions of curcumin, betanin, crystal violet and methylene blue.

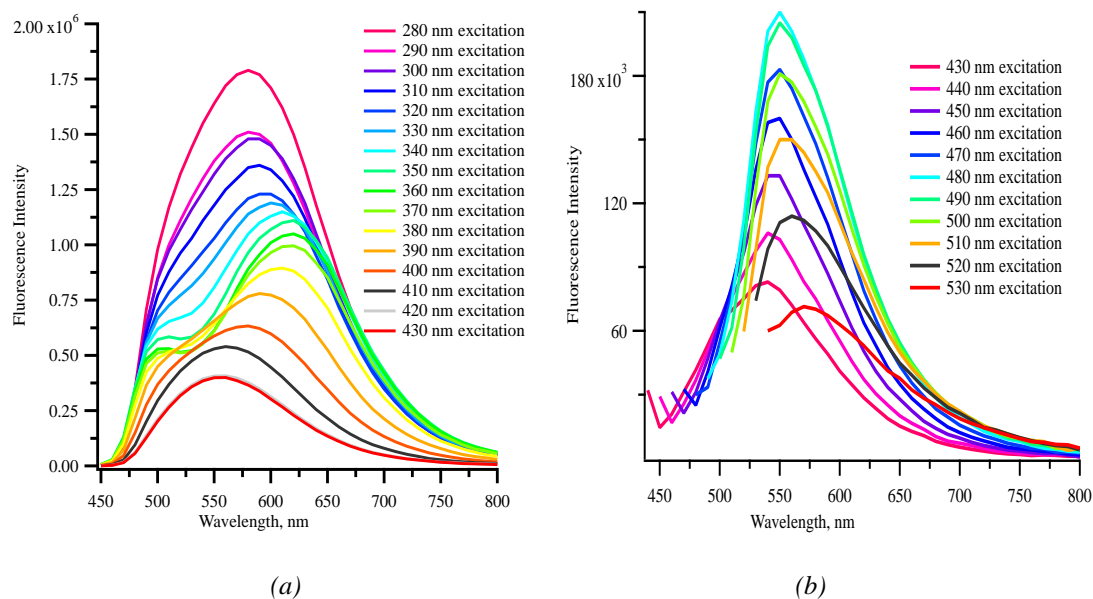


Fig. 6. (a) Fluorescence spectra of ethanolic solution of curcumin and (b) aqueous solution

of betanin as a function of different excitation wavelengths.

For the aqueous solution of betanin, fluorescence intensity gradually increases as the excitation wavelength increases up to 480 nm excitation and then starts to decrease as a function of decrease in excitation wavelength (Fig. 6 (b)). This indicates that the spectral and photochemical properties of some dyes (at least curcumin and betanin) are influenced by the solvents and the excitation wavelengths.

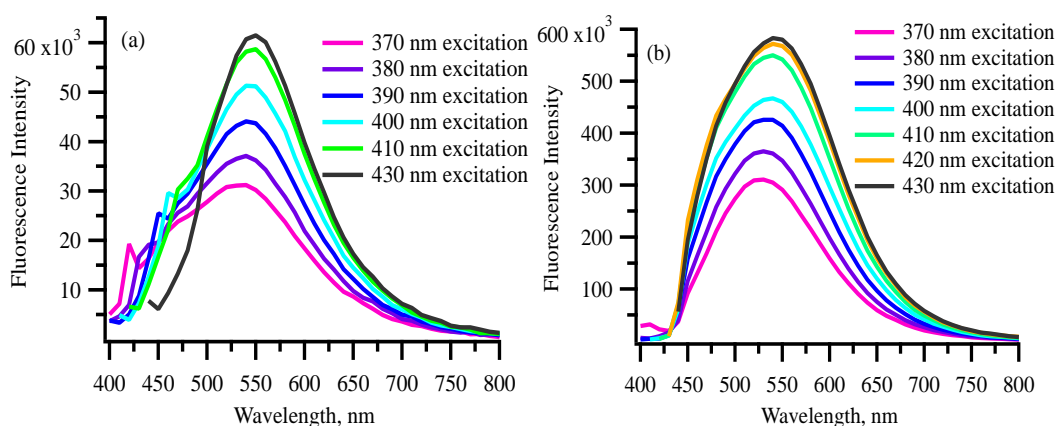


Fig. 7. (a) Fluorescence spectra of aqueous extract and (b) ethanolic extract of turmeric as a function of different excitation wavelengths.

3.4. Computational Studies

In addition to the above-described experiments, we completed theoretical calculations using density functional theory (DFT) and time-dependent density functional theory (TD-DFT) to estimate theoretical band gap energy and to investigate the electronic structure of the dye molecules. We found that the B3LYP functional with 6-311+G (2d, p) basis set provided more accurate electronic transition, HOMO-LUMO energy gaps. Therefore, the geometry optimization and energies of curcumin, betanin, crystal violet and methylene blue dyes were obtained from the B3LYP DFT calculations. The optimized structures are depicted in Fig.8. Curcumin exhibits di-keto and keto-enol (enol) tautomeric forms (Fig. 8). As expected, we found that in both water and ethanol, the di-keto form is more stable than the keto-enolic one by 7.06 kcal/mol and 7.17 kJ/mol respectively. The presence of two phenolic-methoxy groups on the opposite sides of the curcumin backbone is responsible for extra stability for the di-keto tautomer, in which the more polar solvents like water molecules easily stabilize di-keto tautomer through formation of stable complexes via *H*-bonding. However, keto-enolic form is generally more stabilized ($\sim 5\text{-}8 \text{ kcal/mol}$) than the di-keto form in most of the non-polar and moderately polar solvents [38]. The optimized molecular geometry of betanin is shown in Fig. 8, which is a glycoside of betacyanin, having an indole-2- carboxylic acid moiety *N*-linked to a pyridine dicarboxylic acid group through an acetyl group. Similarly, the energy favorable conformation of methylene blue and crystal violet is also depicted in Fig. 8.

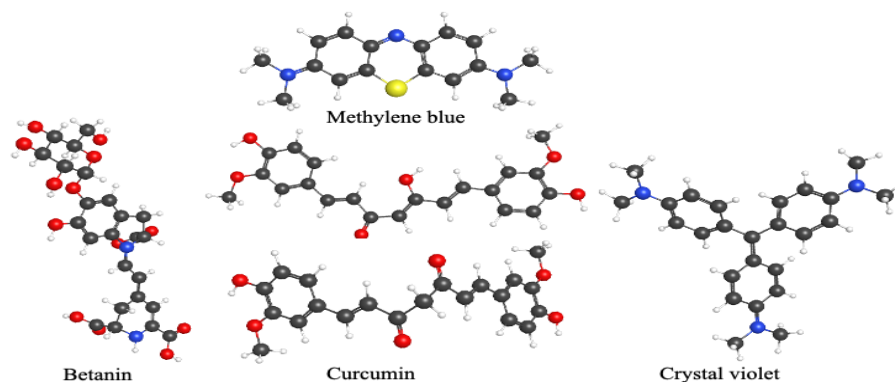


Fig. 8. Optimized structures of curcumin, betanin, crystal violet, and methylene blue.

The HOMO and LUMO energy levels were identified and the optical band gap was calculated by taking the difference between the values of these two energy levels (Fig.9). We found that methylene blue dye in both solvents has the lowest band gap energy (~ 2.435 eV in water and 2.433 eV in ethanol) and curcumin (di-keto) has the highest optical gap of 3.472 and 3.430 eV in both solvents respectively, while curcumin (keto-enol), betanin and crystal violet have optical gap of 3.133 and 3.127 , 2.511 and 2.552 , and 2.698 , 2.697 eV in water and ethanol respectively (Fig. 9). These energy gap values indicate that all of the four dyes can absorb visible light (Figure 3). On photo-excitation, electron density shifts from HOMO level to LUMO level of all dyes.

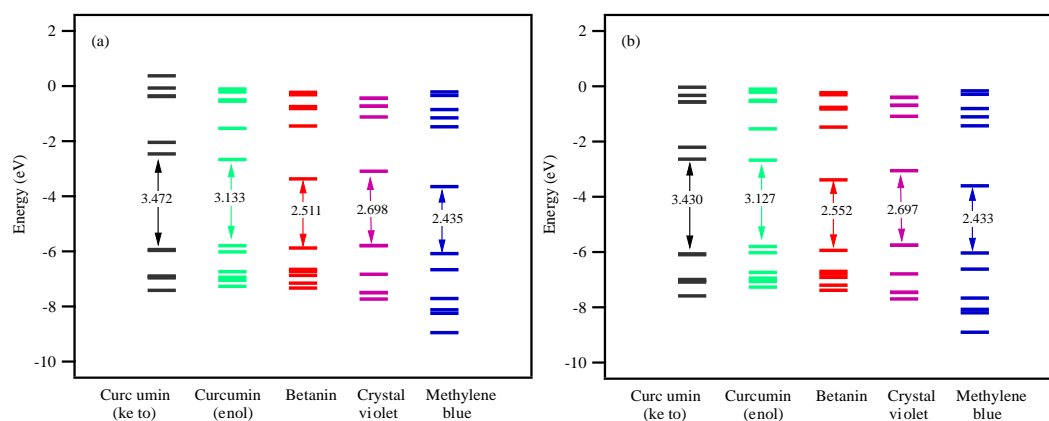


Fig. 9. DFT predicted energy diagrams for curcumin, betanin, crystal violet, and methylene blue (a) in ethanol and (b) in water.

The highest occupied molecular orbital (HOMO) and the lowest unoccupied molecular orbital (LUMO) of the dye molecules are shown in Fig. 10. The analysis of the frontier molecular orbital shows that the HOMO orbitals of curcumin are mainly centralized on the benzene rings and vinyl groups of curcumin, whereas the LUMO orbitals are localized on the unsaturated C=C double bond and oxygen atoms in carbonyl groups (Fig. 10). Thus, π bonds and lone pairs of oxygen atoms are responsible for the charge transfer from HOMO to LUMO in curcumin. In betanin, the probability distribution of the electron density corresponding to the HOMO and LUMO levels is located around the betaine moiety, the betalamic acid group (Fig. 10). Similarly, analyzing the HOMO orbital of crystal violet, we found that its HOMO orbitals chiefly on the C₉=C₁₀ double bond. We noticed that there is a notable increase in electron density on the central carbon in the LUMO (top part of the molecule). We found that methylene blue had its HOMO orbitals mainly localized on the two benzene rings and nitrogen atoms, whereas its LUMO orbitals is predominately delocalized on central sulfur and nitrogen atom.

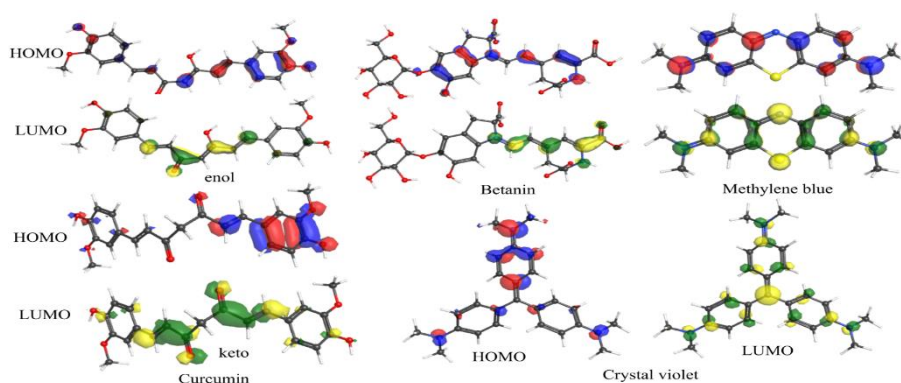


Fig. 10. DFT predicted frontier MOs diagrams for curcumin, betanin, methylene blue, and crystal violet.

As described above, some of the requirements for dye should fulfill in order to be an efficient sensitizer for optimum performance of DSSC. Mainly, the LUMO energy level of the dye molecule should lie energetically above the conduction band of the TiO_2 , and HOMO energy level of the dyes must be positioned below the redox potential of the electrolyte [4,-6]. The band diagram (Fig. 11) shows an appropriate alignment of the energy levels of curcumin, betanin, crystal violet, and methylene blue with respect to those of TiO_2 and the electrolyte. As noted, (Fig. 11) the LUMO levels of the all four dyes are higher than those of the conduction bands of TiO_2 and ITO, which means that excited electrons in the LUMO could inject into the conduction band of the semiconductor. Similarly, the HOMO levels of all the dyes are aligned below the redox potential of the electrolyte could promote dye regeneration (Fig. 11). In general, the interfacial band gap of the acceptor will be larger when the HOMO of the donor becomes lower. Methylene blue (-6.032 eV) has the lowest HOMO among all four dyes. So, we expect that a DSSC with methylene blue would potentially have a higher power conversion efficiency than the DSSCs with other dyes. Moreover, crystal violet seems to have an almost negligible dipole moment ($\sim 0.007 \text{ D}$), indicating that its interaction with TiO_2 may be weak and the charge transfer may not be effective. This could affect the solar cell performance. We will describe this cell performance in detail in the performance test section or power conversion efficiency of the solar cells section.

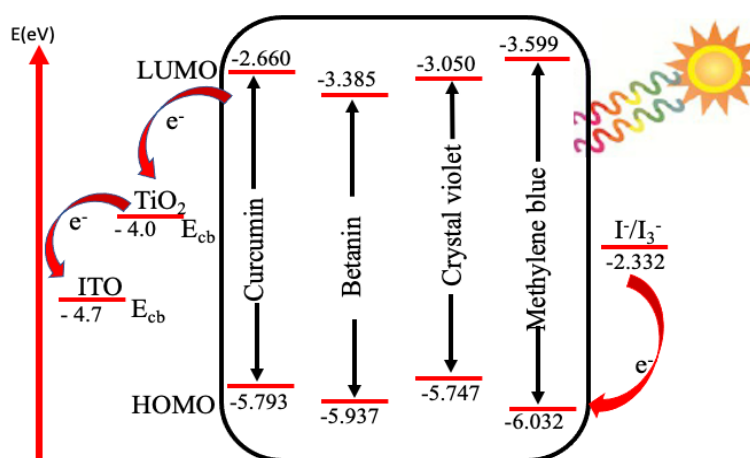


Fig.11. Schematic energy diagram of ITO, TiO_2 , E_{HOMO} , and E_{LUMO} of curcumin, betanin, crystal violet, and methylene blue, and electrolyte (I^-/I_3^-).

We also carried out TDDFT calculations to predict the theoretical absorption spectra of all dyes (Fig. 12 and Figs. S9-S15). The experimental versus predicted absorption spectra of these dye molecules are compared. Overall, we observed good agreement between theory and experimental absorption spectra for all of the dye molecules. For example, as shown in Fig. 12, the TDDFT predicted and the experimental absorbance spectra for betanin in water are in good agreement. In the betanin, the band arise from a HOMO \rightarrow LUMO transition with an energy of ~ 2.39 eV and an oscillator strength $f = 1.0717$. In curcumin, this is a combination of HOMO \rightarrow LUMO and HOMO-1 \rightarrow LUMO transitions with an energy of ~ 2.75 eV and an oscillator strength $f = 1.2267$, while in crystal violet, this is a HOMO-1 \rightarrow LUMO transition with an energy of ~ 2.449 eV and an oscillator strength $f = 0.8098$. Similarly, in methylene blue, it is a HOMO \rightarrow LUMO transition.

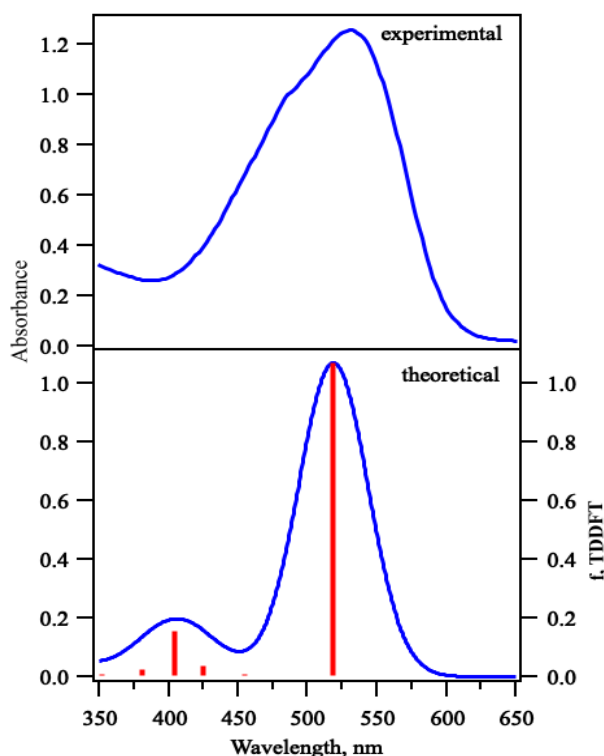


Fig.12. TDDFT predicted UV-vis spectra of betanin in water.

3.5. Performance test (efficiency) power conversion efficiency

Solar cells of seven configurations in each solvent were fabricated (in total 14 solar cells) including: curcumin, betanin, methylene blue, crystal violet, curcumin- crystal violet, betanin- methylene blue, and curcumin-betanin-crystal violet-methylene blue solar cell.

Table 1. Performance characteristics of the solar cells being studied.

Cell	Solvent	V_{oc} (V)	J_{sc} (mA cm^{-2})	Fill factor (FF)	Efficiency (η) (%)
Curcumin	Ethanol	0.39	5.19	0.47	0.95
Betanin	Ethanol	0.56	1.53	0.68	0.58
Mehtylene Blue	Ethanol	0.36	4.42	0.52	0.83
Crystal Violet	Ethanol	0.33	5.09	0.58	0.97
Curcumin + Crystal Violet	Ethanol	0.63	7.48	0.41	1.94
Betanin + Mehtylene Blue	Ethanol	0.40	7.32	0.41	1.21
All	Ethanol	0.61	9.34	0.64	3.63
Curcumin	Water	0.38	2.16	0.52	0.42
Betanin	Water	0.51	3.54	0.57	1.03
Mehtylene Blue	Water	0.39	4.31	0.46	0.77
Crystal Violet	Water	0.36	4.43	0.58	0.92
Curcumin + Crystal Violet	Water	0.47	6.24	0.36	1.06
Betanin + Mehtylene Blue	Water	0.45	7.03	0.43	1.25
All	Water	0.53	8.11	0.60	2.57

The J - V characteristic of the all 14 configurations were studied using homemade solar simulator under a standard $AM1.5G$ illumination condition of 100 mW/cm^2 . The power conversion efficiency of the solar cells was measured in the presence of a mask defining the active area of 0.99 cm^2 . The values of open-circuit voltage (V_{oc}), short-circuit current density (J_{sc}), fill factor (FF), and power conversion efficiency (η) derived from the J - V curves of fourteen samples of each configuration, are listed in Table 1. We did not study turmeric and beetroots based solar cells in this study.

It is evident that ethanolic curcumin-based cell has higher power conversion efficiency (PCE) than aqueous one because of the solubility effect. This solubility effect also affects the $PCEs$ for betanin based cells where aqueous betanin-based cell has higher efficiency than alcoholic one. We found that $PCEs$ for both methylene blue and crystal violet-based solar cells are similar in both solvents, which suggests that $PCEs$ for those solar cells are independent with types of solvent.

When co-sensitized, the performance of the solar cell is better due to an increased current density, which can be attributed to its increased absorption spectrum by the complementary absorbing regions of the various pigments. To determine the optimum sequence of sensitization for the co-sensitized solar cell configurations, the following configurations were fabricated in each solvent system: (i) curcumin followed by crystal violet, (ii) betanin followed by methylene blue, and (iii) mixture of all four dyes. For making the different combination of dyes, we have taken account the absorption spectrum and interaction capacity of each dye molecules. The photovoltaic parameters of all the fabricated cells were evaluated for DSSCs with individual and combined dyes. As shown in Table 1, the $PCEs$ for DSSCs generally increased with the change in the composition of dyes. We found that the curcumin-crystal violet co-sensitized solar cell or betanin-methylene blue co-sensitized solar cells in both ethanol and water have PCE of 1.94 % and 1.21 % and 1.06 % and 1.25%, respectively (Table 1). Table 1 clearly shows that the $PCEs$ of DSSCs with combined dyes (betanin-methylene blue or curcumin-crystal violet co-sensitized) in both solvents are ~ 1.7 times larger than that with the individual dyes. Additionally, photovoltaic parameters were evaluated for DSSCs with four combinations of dyes: curcumin-crystal violet-methylene blue-betanin. As depicted in table 1, the $PCEs$ for DSSCs with four combination of dyes (betanin-methylene blue or curcumin-crystal violet) have larger values than DSSCs with two

combinations of dyes. The highest PCE of 3.63%, with an J_{sc} of 9.34 mA/cm^2 , a V_{oc} of 0.61 V, and a FF of 0.64, was obtained for the combination of all four dyes in ethanol solution, while the PCE of 2.57% with a J_{sc} of 8.11 mA/cm^2 , a V_{oc} of 0.53 V, and a FF of 0.60, was obtained for the combination of all four dyes in water solution (Table 1 and Fig.13). This suggested that the PCEs of DSSCs with four combination of dyes are ~ 2 times larger than that with the two combinations of dyes. As noted already, the better performance of co-sensitized betanin-methylene blue or curcumin-crystal violet or betanin-methylene blue-curcumin-crystal violet cells is due to better matching of the absorption peak of betanin and methylene blue or curcumin and crystal violet and betanin and methylene blue, curcumin and crystal violet with the incident solar spectrum, which was confirmed by UV-vis spectra (Figs. 3 and 4). As shown in Figs. 3 and 4, the absorption spectrum of individual dyes covers only a small range of the solar spectrum, while the combination of dyes covers a wider range of the solar spectrum. This obviously broadened the absorbed light range which ultimately enhanced the power conversion efficiencies. Additionally, J - V characteristic curve of DSSCs based on four combinations of dyes in ethanol and water solutions are depicted in Fig. 13. The PCE for four combinations of dyes-based solar cell in ethanolic solution is greater than that of in aqueous solution. The greater efficiency in ethanolic solution might be attributed by the solubility effect of the dye molecules.

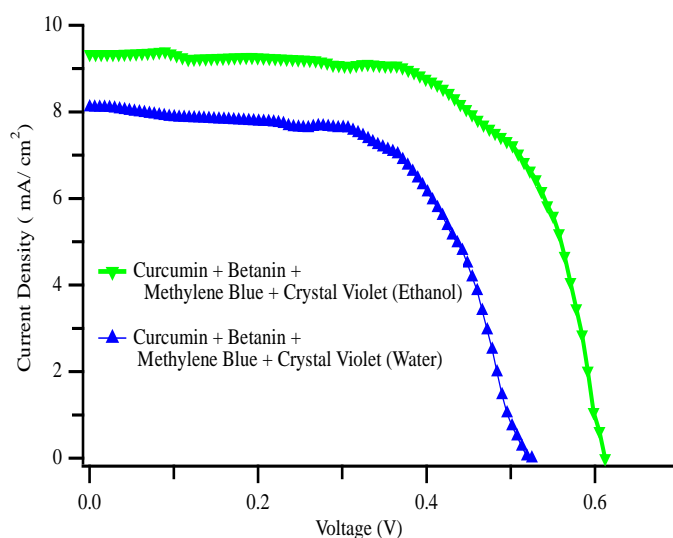


Fig. 13. J - V characteristics of a curcumin, betanin, methylene blue and crystal violet-based solar cell in (a) ethanol, and (b) water.

4. Conclusions

In this research, the novel type of dye-sensitized solar cells based on the combination of four dyes, including curcumin, betanin, crystal violet, and methylene blue, were prepared, and characterized in ethanol and water. Both DFT and TDDFT calculation were carried out to probe the optimized structure and excited properties of these dye molecules. The HOMO and LUMO energies of all dye molecules showed their optimal alignment with respect to the conduction band of the TiO_2 semiconductor and reduction potential energy of the I^-/I_3^- electrolyte. The fabrication of each individual and combination of dyes based solar cells was optimized, and the performance characteristics were evaluated and compared. We found that DSSC with four combination of dyes (curcumin, betanin, crystal violet, and methylene blue in ethanol) has the highest power conversion efficiency (PCE) of 3.63% than in water (PCE of 2.57 %). This may be attributed to the more optimal alignment of energy levels of all dye molecules and solubility effect in ethanol as compared to in water.

Acknowledgements

This work was supported by the Indiana Academy of Science (IASSG-S21-03) and the Department of Chemistry, Earlham College, Richmond, IN.

References

- [1] N. Kannan, D. Vakeesan, *Renew Sustain Energy Rev.* 62, 1092 (2016); <https://doi.org/10.1016/j.rser.2016.05.022>
- [2] N.S. Lewis, *Science* 315 (5813),798 (2007); <https://doi.org/10.1126/science.1137014>
- [3] M.M. Halmann, M. Steinbert, "greenhouse gas carbon dioxide mitigation", *Science and Technology*, CRC Press, USA 1998; <https://doi.org/10.1201/9781482227833>
- [4] D. Wang, W. Wei, Y.H. Hu, *Ind. Eng. Chem. Res.* 59 (22), 10457 (2020); <https://doi.org/10.1021/acs.iecr.0c00612>
- [5] A.M. Ammar, H.S.H. Mohamed, M. M. K. Yousef, G.M. Abdelhafez, A. S. Hassaniien, A. S. G. Khalil, *J. Nanomater.* 2019, 1 (2019); <https://doi.org/10.1155/2019/1867271>
- [6] C. Lin, Y. Liu, G. Wang, K. Li, H. Xu, W. Zhang, C. Shao, Z. Yang, *ACS Omega* 6 (1) 715 (2021); <https://doi.org/10.1021/acsomega.0c05240>
- [7] G.F. Brown, J. Wu, *Laser Photonics Rev.* 3, 394 (2009); <https://doi.org/10.1002/lpor.200810039>
- [8] R.L. Hirsch, *Energy Policy* 36 (2), 881 (2008); <https://doi.org/10.1016/j.enpol.2007.11.009>
- [9] D. Chapin, C. Fuller, G. Pearson, *J. Appl. Phys.* 25(5), 676 (1954); <https://doi.org/10.1063/1.1721711>
- [10] B. O'Regan, M. Gratzel, *Nature*, 353, 737 (1991); <https://doi.org/10.1038/353737a0>
- [11] C. Bechinger, S. Ferrere, A. Zaban, J.Sprague, B.A. Gregg, "Photo -electrochromic Windows and Displays". *Nature* 383, 608 (1996); <https://doi.org/10.1038/383608a0>
- [12] J. Gong, K. Sumathy, Q. Qiao, Z. Zhou, *Renew. Sustain. Energy. Rev.* 68, 234 (2017); <https://doi.org/10.1016/j.rser.2016.09.097>
- [13] K. Yoo, J.-Y.Kim, J. A. Lee, J.S. Kim, D-K. Lee, K. Kim, J.Y. Kim, B. Kim, H. Kim, W. M. Kim, J.H. Kim, M. J. Ko, *ACS Nano.* 9, 3760 (2015); <https://doi.org/10.1021/acsnano.5b01346>
- [14] M.J. Yun, S.I. Cha, S. H. Seo, H. S. Kim, D.Y. Lee, *Sci. Rep.* 5, 11022 (2015); <https://doi.org/10.1038/srep11022>
- [15] M. Gratzel, *J. Photochem. Photobiol. C: Photochem. Rev.* 4, 145 (2003).
- [16] L. Saadoun, J. A. Ayllon, J. Jimenez-Becerril, J. Peral, X. Domenech, R. Rodriguez-Clemente, *Materials Research Bulletin* 35 (2), 193 (2000); [https://doi.org/10.1016/S0025-5408\(00\)00204-X](https://doi.org/10.1016/S0025-5408(00)00204-X)
- [17] J. Bisquert, J. García-Cañadas, I. Mora-Seró, E. Palo- mares, *Proceedings of the SPIE*, 07 August, San Diego 2003, pp. 49-59.
- [18] M.K. Nazeeruddin, P. Pechy, T. Renouard, S.M. Za- keeruddin, R. Humphry-Baker, P. Comte, P. Liska, L. Cevey, E. Costa, V. Shklover , L. Spiccia, G. B. Deacon, C. A. Bignozzi, M. Gratzel, *J. Am. Chem. Soc.* 123, 1613 (2001); <https://doi.org/10.1021/ja003299u>
- [19] S. Hao, J. Wu, Y. Huang, J. Lin, *Solar Energy* 80, 209 (2006); <https://doi.org/10.1016/j.solener.2005.05.009>
- [20] M. I. Kimpa, M. Momoh, K.U. Isah, H.N. Yahya, M. M. Ndamitso, *Mater. Sci. Appl.* 3, 281 (2012).
- [21] S. Kim, J. K. Lee, S. O. Kang, J. J. Ko, J. H. Yum, S. Fan- tacci, F. De Angelis, D. Di Censo, M. K. Nazeeruddin, M. Gratzel, *J. Am. Chem. Soc.* 128, 16701 (2006); <https://doi.org/10.1021/ja066376f>
- [22] M. K. Kashif, M. Nippe, N.W.Duffy, C.M. Forsyth, C.J. Chang, J. R. Long, L. Spiccia, U. Bach, *Angew. Chem. Int. Ed.* 52, 5527 (2013); <https://doi.org/10.1002/anie.201300070>

- [23] S. Sarwar, K.W. Ko, J. Han, C.H. Han, Y. Jun, S. Hong, *Electrochimica Acta* 245, 526 (2017); <https://doi.org/10.1016/j.electacta.2017.05.191>
- [24] A. Sedghi, H. N. Miankushki, *Int. J. Electrochem. Sci.* 10, 3354 (2015).
- [25] J. Uddin, J. M.M.I. Islam, S. M.K. Khan, E. Hoque, M. A. Khan, *International Letters of Chemistry, Physics and Astronomy* 39, 78 (2014); <https://doi.org/10.18052/www.scipress.com/ILCPA.39.78>
- [26] D. Sengupta, B. Mondal, K. Mukherjee, *Spectrochim. Acta A*, 148, 85 (2015); <https://doi.org/10.1016/j.saa.2015.03.120>
- [27] A. Georgescu, G. Damache, M. A. Gîrțu, *J. Optoelectron. Adv. Mater.* 10, 2996 (2008).
- [28] G. Calogero, G. Di Marco, *Sol. Energy Mater. Sol. Cells*, 92, 1341 (2008); <https://doi.org/10.1016/j.solmat.2008.05.007>
- [29] W. Kohn, L. J. Sham, *Phys. Rev. A* 140, 1133 (1965); <https://doi.org/10.1103/PhysRev.140.A1133>
- [30] A.D. Becke, *J. Chem. Phys.* 98, 5648 (1993); <https://doi.org/10.1063/1.464913>
- [31] C. Lee, W. Yang, R.G. Parr, *Phys. Rev. B* 37, 785 (1988); <https://doi.org/10.1103/PhysRevB.37.785>
- [32] A. D. McLean, G. S. Chandler, *J. Chem. Phys.* 72, 5639 (1980); <https://doi.org/10.1063/1.438980>
- [33] J. Tomasi, B. Mennucci, R. Cammi, *Chem. Rev.* 105, 2999 (2005); <https://doi.org/10.1021/cr9904009>
- [34] M.J. Frisch, G. W. Trucks, H.B. Schlegel, et al. *Gaussian 16*, Revision A.03 (2016).
- [35] D. Zhang, S. M. Lanier, J. A. Downing, J. L. Avent, J. Lum, J. L. McHale, *J. Photochem. Photobiol. A* 195 (1), 72 (2008); <https://doi.org/10.1016/j.jphotochem.2007.07.038>
- [36] G. Calogero, J-H. Yum, A. Sinopoli, G. D. Marco, M. Gratzel, M. K. Nazeeruddin, *Solar Energy* 86, 1563 (2012); <https://doi.org/10.1016/j.solener.2012.02.018>
- [37] F. Jasim, F. Ali, *Microchemical Journal* 46 (2), 209 (1992); [https://doi.org/10.1016/0026-265X\(92\)90040-A](https://doi.org/10.1016/0026-265X(92)90040-A)
- [38] K. I. Priyadarsini, K.I, *Molecules*, 19, 20091-20112 (2014); <https://doi.org/10.3390/molecules191220091>